Metrol. Meas. Syst., Vol. XXII (2015), No. 3, pp. 403–416.

PAN POLSKA AKADEMIA NAUK

METROLOGY AND MEASUREMENT SYSTEMS

Index 330930, ISSN 0860-8229

www.metrology.pg.gda.pl

M&MS

ACCURATE FREQUENCY ESTIMATION BASED ON THREE-PARAMETER SINE-FITTING WITH THREE FFT SAMPLES

Xin Liu[1,2], Yongfeng Ren[1], Chengqun Chu[1], Wei Fang[1]

1) North University of China, National Key Laboratory for Electronic Measurement and Technology, Taiyuan, 030051, China (✉ omol66@163.com, +86 186 0351 4828, *renyongfeng@nuc.edu.cn, chuchengqun@126.com, fangwei@nuc.edu.cn)*

2) Taiyuan University of Science and Technology, College of Electronics and Information Engineering, Taiyuan 030024, China

Abstract

This paper presents a simple DFT-based golden section searching algorithm (DGSSA) for the single tone frequency estimation. Because of truncation and discreteness in signal samples, Fast Fourier Transform (FFT) and Discrete Fourier Transform (DFT) are inevitable to cause the spectrum leakage and fence effect which lead to a low estimation accuracy. This method can improve the estimation accuracy under conditions of a low signal-to-noise ratio (*SNR*) and a low resolution. This method firstly uses three FFT samples to determine the frequency searching scope, then – besides the frequency – the estimated values of amplitude, phase and dc component are obtained by minimizing the least square (LS) fitting error of three-parameter sine fitting. By setting reasonable stop conditions or the number of iterations, the accurate frequency estimation can be realized. The accuracy of this method, when applied to observed single-tone sinusoid samples corrupted by white Gaussian noise, is investigated by different methods with respect to the unbiased Cramer-Rao Low Bound (CRLB). The simulation results show that the root mean square error (RMSE) of the frequency estimation curve is consistent with the tendency of CRLB as *SNR* increases, even in the case of a small number of samples. The average RMSE of the frequency estimation is less than 1.5 times the CRLB with *SNR* = 20 dB and *N* = 512.

Keywords: frequency estimation, CRLB, three-parameter sine-fitting, RMSE, golden section.

1. Introduction

The frequency estimation of sine wave of a digital signal as an important area of research in modern signal processing has been applied in the fields of power systems [1], dynamic characterization of devices and circuits [2], biomedicine [3], optical metrology [4]. Although DFT is very effective and, in the case of FFT, fast enough to be applied in real-time applications, it may become very inaccurate at the non-coherent sampling because of the spectral leakage phenomena [5−6]. It is well known that an *N*-point DFT is calculated for the data length of *N* samples leading to a resolution $2\pi/N$ of the frequency estimation. Frequency estimators mainly include non-iterative IpDFT algorithms and iterative DFT-based algorithms [7]. Generally, a two-stage search can be implemented to improve the frequency estimation. First, a coarse estimation is usually performed by an *N*-point FFT to locate the index of the largest magnitude. Secondly, a fine search is executed around the vicinity of the index. Several alternative search methods such as IpDFT or iterative methods for the second stage were reviewed in [8].

IpDFT with the Agrež algorithm [9] and IpDFT with the Yoshida algorithm [10] were described in [8]. In [11], Rife and Vincent proposed an estimator, which is called the Rife algorithm with a two-point interpolated DFT for the frequency estimation of a sinusoidal signal. In order to improve the estimation accuracy, a modified Rife algorithm (MRife) [12−13] was proposed based on applying FFT twice, by moving the signal frequency to the midpoint of two neighboring discrete frequencies.

Article history: received on Dec. 17, 2014; accepted on May 06, 2015; available online on Sep. 21, 2015; DOI: 10.1515/mms-2015-0032.

In [14], many iterative DFT-based methods of frequency estimation were reviewed, which involved a parametric STMB iterative algorithm [15], an interpolated DFT BY1 algorithm with leakage correction [16], *etc*.

This paper presents a simple DFT-based golden section searching algorithm (DGSSA) for the single tone frequency estimation by minimizing the LS error of three-parameter sine fitting. DGSSA is a two-stage process. Firstly, the DFT of the sampled sequence is calculated, and the fine searching scope is determined. In the second stage, the golden section searching algorithm is adopted for fine searching of the estimated frequency. Moreover, it is proved that the root mean square error (RMSE) of the proposed frequency estimator is consistent with the tendency of CRLB as *SNR* increases by comparing with different estimation algorithms.

2. Frequency estimation with sine fitting algorithm

2.1. Signal model

A single tone frequency sinusoidal signal observed under white Gaussian noise can be modeled in the four-parameter sine fitting as follows:

$$y(n)=x(n)+e(n)=A_v\cos(\omega\cdot n\cdot\Delta t+\varphi)+C+e(n)\quad (n=0,1,\cdots,N-1), \tag{1}$$

where A_v, $\omega = 2\pi f_c$, φ and C are the amplitude, angular frequency, initial phase and dc component, which are all unknown, respectively [17]. The error term $e(n)$ which consists of observation noise, quantization noise, parameter inaccuracies, *etc*. [18] is modeled as a zero mean white Gaussian stochastic process with variance σ^2. The Gaussian assumption is crucial to the validity of the theoretical results derived in this paper and may seem restrictive. In many practical cases where the measurement noise is independent of the signal $x(n)$, the Gaussian assumption is a reasonable approximation, and the least-squares approximation is valid [19]. N samples ($y_0, y_1, \ldots\ldots, y_{N-1}$) are acquired at sampling time:

$$t_n=\frac{n}{f_s}\quad (n=0,1,\cdots,N-1). \tag{2}$$

The sampling frequency f_s is assumed to be larger than $2*f_c$ to satisfy the Nyquist Theorem. The relationship between the frequencies f_c and f_s is equal to:

$$\frac{f_c}{f_s}=\frac{M}{N}=\frac{J+\delta}{N}, \tag{3}$$

where M presents the number of sample cycles, in general being a not-integer value. J and δ ($-0.5 \le \delta < 0.5$) are the integer and fraction parts of M, respectively. If the sine wave is sampled coherently, then $\delta = 0$ and the phase difference between two adjacent samples is equal to $2\pi/N$. Most of the four-parameter sine fitting are applied in parameter estimation under the assumption of coherent sampling. However, in practice, such a condition can never be perfectly met since the true value of signal frequency f_c is unknown. When non-coherent sampling occurs, we have $\delta \neq 0$.

2.2. Four-parameter sine fitting

Three-parameter sine fitting procedures have been standardized in the IEEE Standard 1057 [20] and 1241 [17]. The amplitude, phase and dc component of the acquired samples can be estimated accurately in the three-parameter fitting by a non-iterative procedure, assuming that the sine frequency is known. However, in the four-parameters fitting, the above three parameters and frequency of the input sine wave are all unknown. The iterative method begins with the initial frequency estimation, and the fitting equations are nonlinear.

Equivalently, the observed data $y(n)$ in (1) are expressed as:

$$y(n) = A\cos(2\pi f_c \cdot t_n) + B\sin(2\pi f_c \cdot t_n) + C + e(n), \tag{4}$$

where $A = A_v\cos\varphi$ and $B = -A_v\sin\varphi$ are the amplitudes of the in-phase and in-quadrature components in Volt, respectively. C and f_c are the dc component in Volt and the frequency of input sine in Hertz, respectively. Therefore, the initial phase can be expressed as:

$$\varphi = \begin{cases} \arctan(\frac{-B}{A}) & A \geq 0 \\ \arctan(\frac{-B}{A}) + \pi & A < 0 \end{cases}. \tag{5}$$

We intend to estimate the sine wave that best fits, in a least square (LS) error sense, to these N samples. The phase φ is considered to be a random variable uniformly distributed within an interval of 2π. In general, the four-parameter sine fitting algorithm needs an initial value of the estimated frequency f_0. Then it uses the following matrix and vector:

$$D(f_0) = \begin{bmatrix} \cos(2\pi f_0 t_0) & \sin(2\pi f_0 t_0) & 1 \\ \cos(2\pi f_0 t_1) & \sin(2\pi f_0 t_1) & 1 \\ \cdots & \cdots & \cdots \\ \cos(2\pi f_0 t_{n-1}) & \sin(2\pi f_0 t_{n-1}) & 1 \end{bmatrix}, \quad Y = \begin{bmatrix} y(0) \\ y(1) \\ \cdots \\ y(n-1) \end{bmatrix}. \tag{6}$$

Since from (4) the following relation is fulfilled: $Y = D^*[A; B; C]$, (7) follows if matrix $D(f_0)$ is of full rank:

$$\theta = \begin{bmatrix} A \\ B \\ C \end{bmatrix} = (D^T D)^{-1}(D^T Y). \tag{7}$$

Then the LS error can be calculated and shown in (8) as:

$$\varepsilon(n) = \frac{1}{N}\sum_{n=0}^{N-1}\left[y(n) - A\cos(2\pi f_0 \cdot t_n) - B\sin(2\pi f_0 \cdot t_n) - C\right]^2). \tag{8}$$

By minimizing the LS error in (8) with respect to the vector θ, the best estimated $\hat{\theta}$ of the sine-wave parameter vector θ is obtained.

The four-parameter sine fitting is linear only when the frequency is known. Otherwise, it is nonlinear. Therefore, the four-parameter sine fitting, started from different initial frequency estimation values, may converge on different local minima and lead to a large estimation error. If the initial frequency f_0 is accurate, the minimum LS error can be obtained; otherwise the error will be large. So, the accuracy of the estimated value of initial frequency f_0 is very important for the convergence of the four-parameter fitting. The normalization error curves of the four-parameter sine fitting of different numbers of observed cycles are shown in Fig. 1.

In Fig. 1, the LS error of the four-parameter sine fitting as a function of frequency ratio (f_0/f_c) was calculated for different numbers of oscillation cycles(periods) per one DFT, M = 0.6, 0.8, 1, 3, 5 and 10, respectively. The frequency of input sine wave is set to 2.012342 Hz which is sampled at 100 S/s. It can be concluded that, when the estimated value of initial frequency is infinitely close to the true value, the normalization LS error is minimized. That is to say, the four-parameter sine fitting is convergent. However, a slight shift in the frequency causes an increase of the LS error because the frequency mismatch changes the phase of all the reconstructed sine wave points, making all the points add to the LS errors. Taking into account the multiple periods of samples, a small frequency shift can cause a large error because it causes the $N*\Delta f$ frequency for all the recorded samples, cumulatively. The error increases depending on the contributions to the RMS signal value.

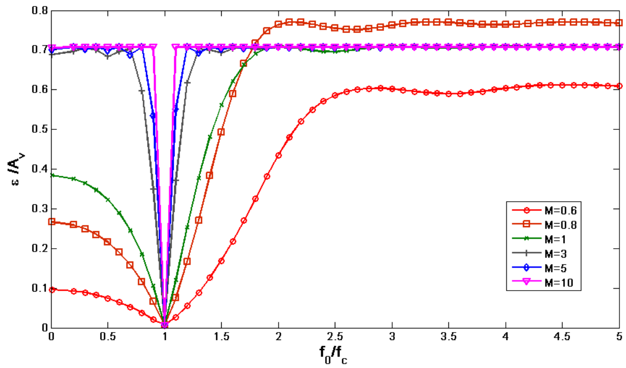

Fig. 1. The normalization LS error versus frequency ratio (f_0/f_c) for different numbers of oscillation cycles.

In addition, beyond the range of $(f_{k_0} - \frac{f_s}{N},\ f_{k_0} + \frac{f_s}{N})$, the maxima of LS error are approximately equal to 0.7, when $M > 1$. k_0 is the index of the maximum of the DFT spectrum. In this scope, there is only one minimum value of LS error corresponding with the frequency [21].

Most of frequency estimation algorithms based on DFT consist of two stages, which are the coarse estimation and the fine estimation. In the first stage, the DFT of the time series is calculated, with the frequency accuracy of Δf which is equal to f_c/N. In the second stage, by using different interpolation strategies, the frequency deviation $\hat{\delta}$ between the true frequency and k_0 is estimated. If no window is used, the exact (9) is adopted to estimate the frequency by the interpolated DFT. Our goal in this paper is to calculate $\hat{\delta}$.

$$\hat{f} = (k_0 + \hat{\delta}) \cdot \Delta f \quad (k_0 = 0, 1, \cdots N-1; -0.5 \le \hat{\delta} < 0.5). \tag{9}$$

IEEE1241 requires that at least four periods of the sine wave are recorded [22]. In order to avoid getting into local minima, it can be made possible that the proposed algorithm works well even throughout as few periods of the record length as possible.

3. Proposed DFT-based golden section searching algorithm (DGSSA)

3.1. Optimizing golden section searching range

In one-dimensional linear searching problems, several searching strategies are used to determine the search steps, such as a binary search, the Newton's method, and a golden section. As shown in Fig. 2, because the optimal point ($f_0/f_c = 1$) is unique in the sense of the frequency range, it is a unimodal optimization problem. The first and second derivatives are required in the Newton's method; however, the all-order derivatives of the normalization LS error of the three-parameter fitting algorithm at different frequency points are difficult to calculate. So, the Newton's method is not suitable. The golden ratio search has been thought the best for the uni-modal optimization [23]. In addition, the convergence ratio of the binary search is lower than that of the golden section, which has a higher convergence speed. In this paper the golden section is adopted to find the optimal frequency through minimization of the LS error, as shown in (8) with a straight search.

In recent years, the golden section has been applied to optimize timings of traffic signal systems with good results [24]. As shown in [25], the golden ratio is introduced to enhance the local search of simple genetic algorithms. Two local optimums tend to the same pit of the solution space. It is assumed that there is a potentially better estimation value between the two local optimums. So, the location of local optical optimized values can be identified by the golden ratio, that is to say, two boundary value locations of the golden section searching algorithm can be determined.

In the coarse estimation stage, an N-point DFT of x(n) is calculated, as shown in Fig. 2. The peak value $X[k_0]$ – as shown in (10) – in the DFT magnitude spectrum is expected to be around the true frequency f_c, represented by the blue symbol □.

$$X[k]=\sum_{n=0}^{N-1}x[n]e^{-j(2\pi/N)nk},\qquad k_0=\arg\max_k\left|X[k]\right|. \tag{10}$$

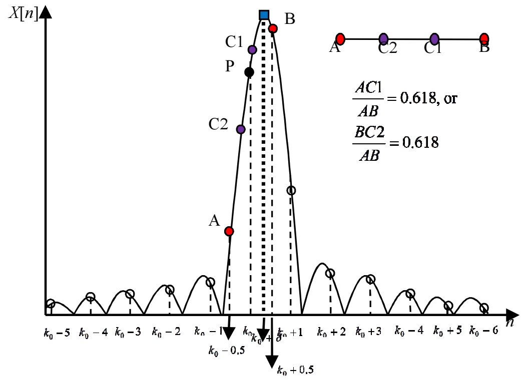

Fig. 2. The magnitude spectrum of the sine wave with DFT.

As shown in Fig. 2, it can be assumed that the maximum spectral line obtained by DFT of the frequency is point P. The adjacent spectral lines $X[k_0 - 0.5]$ and $X[k_0 + 0.5]$ in relation to $X[k_0]$ are marked point A and B as:

$$X[k_0-0.5]=\sum_{n=0}^{N}x(n)\exp(-j2\pi\frac{k_0-0.5}{N}n), \tag{11}$$

$$X[k_0+0.5]=\sum_{n=0}^{N}x(n)\exp(-j2\pi\frac{k_0+0.5}{N}n). \tag{12}$$

Because δ of the true frequency satisfies the relation ($-0.5 \le \delta < 0.5$), the true frequency is located within the range of $[(k_0-0.5)\cdot\frac{f_s}{N},(k_0+0.5)\cdot\frac{f_s}{N})$. According to the golden ratio, it is assumed that the potential local frequency is C1 or C2, that is, the relationship between the segment AC1 and the segment AB satisfies the golden ratio definition. In addition, the relationship between the segment BC2 and the segment AB also satisfies the golden ratio definition.

In Fig. 3, the normalized LS RMSE of the three-parameter algorithm is plotted against the index of DFT samples. The red mark ○ indicates the RMSE corresponding with the frequency estimated by DFT, the green mark □ indicates the RMSE corresponding with the frequency estimated by the proposed algorithm. It is seen that, by using a sine with $f_c = 20.09375$ MHz, $f_s = 100$M Hz, $SNR = 20$ dB, $N = 32$, the four-parameter sine fitting LS error ε is larger when using DFT to estimate the initial frequency. By the optimized frequency searching algorithm proposed in this paper, frequency accurate result is determined.

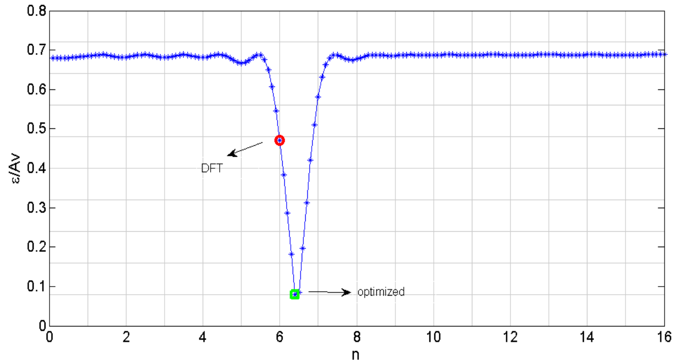

Fig. 3. The normalized LS RMSE of the three-parameter algorithm as a function of the index of DFT sample.

3.2. DFT-based golden section searching algorithm

In the DGSSA algorithm the sine-wave frequency estimation can be found by looking for the index of (10), *i.e.*, of the discrete-time Fourier transform (DtFT). When the search domain is reduced by (11–12), *e.g.* by using the Newton's search, the strategy is replaced by the golden-ratio division. The paper presents an original, new solution for the precise estimation of single sinusoid parameters (frequency, amplitude, phase, DC). The method consists of the following steps:

1) The initial frequency estimate is calculated by using an N-point DFT and setting a stop condition p or the number of iterations I.
2) According to the value of k_0, there are two cases in determining the left and right border frequencies $F(l)$ and $F(r)$ by making use of k_0-index of max(abs()) value of DFT:
   a) If $k_0 \neq 0$, then $F(l) = f_{k_0-0.5} = \Delta f \cdot (k_0 - 0.5)$ and $F(r) = f_{k_0+0.5} = \Delta f \cdot (k_0 + 0.5)$.
   b) If $k_0 = 0$, then $F(l) = \Delta f \cdot \xi$ and $F(r) = f_{k_0+0.5} = \Delta f \cdot (k_0 + 0.5)$. ξ is the coefficient of F(l) which is small enough to ensure $F(l) < f_c$, for example 10^{-5}.
3) Then, the golden division is applied and two inner frequencies F(m) and F(t) are calculated – inner with respect to $F(l)$ and $F(r)$.
4) For these frequencies the model (amplitude, phase and DC) fitting to the signal is done – (7) – and the LS fitting errors $\varepsilon(m)$ and $\varepsilon(t)$ are calculated.
5) According to ε(m) and ε(t) values of frequencies $F(m)$ and $F(t)$, $F(m)$ and $F(t)$ are modified and "flag" is set (0 or 1) (step 8).
6) Again, the three-parameter sine fitting (amplitude, phase, DC) is done and the errors $\varepsilon(m)$ and $\varepsilon(t)$ are calculated.
7) If $|F(r) - F(l)| >$ p or I < I, go to (4); otherwise continue.
8) $f_c = F(m)$ or $F(t)$ according to the "flag" value (0 or 1).

In order to improve the estimation accuracy, changes of the algorithm in fine searching are proposed, as shown in the above process. The amplitudes, phases and dc components are recalculated after the frequency is adjusted by the three-parameter sine fitting to ensure that the corrected signal model is being used in each updating process in the above steps (4) and (5) for the new frequency searching range.

The frequency updating procedure is shown in Fig. 4.

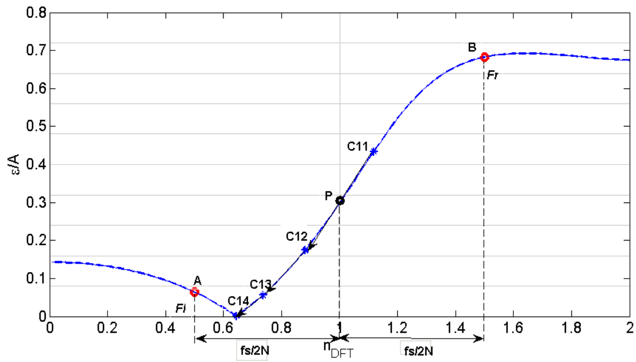

Fig. 4. The updating process of the corrected frequency in each update of the frequency scope by DGSSA on the condition of sine-wave frequency $f_c = 2.012342$ Hz, sampling frequency $f_s = 100$ Hz; $N = 32$. The initial boundaries are $F(l)$ and $F(r)$, respectively.

As shown in Fig. 4, by calculating the N-point DFT of observed samples, two border frequencies $F(l)$ and $F(r)$ are obtained. The frequencies are used according to step (4) as the input to perform the three-parameter fitting algorithm. By comparing the RMSE values of $F(m)$ and $F(t)$ the first corrected frequency C11 is obtained. The decreased scope is updated to the range of A to C11. The RMS errors of updated $F(m)$ and $F(t)$ are recalculated, then the second corrected frequency C12 is obtained, and so on.

It can be seen from Fig. 4, that the corrected frequency is close to the minimum from the initial scope after running the procedure only 4 times. Because there is only one extreme point in the searched region, the searched scope is decreased gradually. By setting a stop condition or the number of iterations reasonably, the global convergence can be obtained.

3.3. Cramer-Rao Lower Bound

The CRLB is the lower bound on the covariance of any unbiased estimation. The CRLB of the estimated frequency using IEEE Standard 1057 is derived in [19].

$$CRLB(\hat{f}) \approx \sqrt{\frac{6\sigma^2}{(\pi T_s)^2 \cdot N \cdot (N^2-1) A_v^2}} = \sqrt{\left(\frac{f_s}{2\pi}\right)^2 \frac{12}{SNR \cdot N \cdot (N^2-1)}}, \tag{13}$$

where SNR is defined as $SNR = \frac{A_v^2}{2\sigma^2}$, A_v is the amplitude of the sine wave and σ^2 is the variance of the noise.

4. Numerical comparisons

For all simulations in Section 4, the signal is modeled as:
$y(n) = A_v \cos\varphi \cdot \cos(2\pi f_c t_n) - A_v \sin\varphi \cdot \cos(2\pi f_c t_n) + C + e(n)$.

The signal model parameters are set: $A_v = 5$ V, $C = 0$ V, and phase φ which is uniformly distributed over $[0, 2\pi)$ rad. $e(n)$ is the white Gaussian noise added to the signals. All simulation experiments were implemented using MATLAB r2008a, and run on a personal computer with

Intel(R) Core (TM) I3, CPU 1.8G Hz, 4.00 GB memory, and the Microsoft Windows7 operation system. In our experiments, three goals will be pursued and attained. The first goal is to test the accuracy and convergence feature of the proposed method. The second objective is to verify its immunity to the white Gaussian noise. The third goal is to test the impact of the number of samples on the accuracy and computational complexity. To ensure good estimations of the frequency in the presence of additive white Gaussian noise, in accordance with the Monte Carlo method, each value has been averaged over 1000 times. Comparisons of the performance of the proposed DGSSA method with the recent representative frequency estimation methods including Rife [11], MRife [13], BY1 with leakage correction [16], the iterative Steiglitz-McBride (STMB) extension of the Prony algorithm [15], Yoshida IpDFT [10], IpDFT with HANNING window algorithm and the CRLB, are performed.

4.1. Estimation accuracy and convergence of DGSSA

To verify the accuracy of the proposed procedure, signals with a random uniformly distributed phase from 0 to 2π were considered. In this analysis, comparisons are made among DGSSA for 5 iterations (DGSSA, I = 5) and 15 iterations (DGSSA, I = 15), Rife, MRife, BY1 with leakage correction for 5 iterations (BY1-LC, I = 5) and 15 iterations (BY1-LC, I = 15), the iterative Steiglitz-McBride (STMB) extension of the Prony algorithm for 5 iterations (STMB, I = 5) and 15 iterations (STMB, I = 15), Yoshida IpDFT, IpDFT with HANNING window algorithms and the CRLB to validate usefulness of the proposed estimator. For each random phase, 1000 estimations are taken to calculate with SNR = 20 dB. In this section, the sampling frequency is 100 MS/s. The number of observed samples is N = 512, and J = 100. Fig. 5 presents the mean value of the estimation error (estimation bias) as a function of δ varied within [–0.5, 0.5) with the increment of 0.05. Fig. 6 and Fig. 7 depict the RMSE and the maximum modulus of the absolute error of δ estimation under the same simulation conditions.

The frequency estimation is a nonlinear estimation problem; therefore, it is not surprising that all estimators, including the proposed one, are biased. Among non-iterative DFT-based methods, the poorest bias and RMSE belongs to the Rife method which is well known in the literature [13]. Fig. 5 clearly shows that the Rife method has the same precision as the MRife method when $|\delta| > 0.3$. As δ moves towards the centre of the sliding interval, performance of the Rife method is worsened rapidly. The estimators by Yoshida IpDFT, IpDFT with HANNING window algorithm have the similar bias value and RMSE in the absence of noise. Compared with the MRife, Hann window and Yoshida IpDFT methods, the proposed DGSSA with 15 iterations has a lower estimation error. In DGSSA, a high accuracy is obtained by increasing the iteration time. Fig. 6 and Fig. 7 clearly show that, for the STMB and BY1-LC methods, increasing the number of iterations does not improve their performance remarkably. As $|\delta|$ increases, the RMSE and absolute error of BY1-LC for the frequency estimation increase, too. However, with fewer iterations, DGSSA has a lower estimation accuracy. That is because the value of iteration step of DGSSA is a constant value. Conversely, by using 15 iterations, DGSSA has the similar estimated accuracy as STMB. It is also seen that the performance of DGSSA is not affected by the initial phase. The average value of RMSE can be approximately 1.4 times higher than the CRLB.

In order to analyze the convergence feature of DGSSA, sine wave signals with a random uniformly distributed phase are fitted by DGSSA, BY1-LC and STMB, respectively. Fig. 8 shows the convergence of the algorithms versus the number of iterations for N = 1024, SNR = 20 dB, J = 57, δ = 0.24 and f_s = 100 MS/s. For each iteration procedure, 1000 simulations were realized.

Figure 8 shows that for BY1-LC, the number of iterations has the minimal impact on its performance. With the STMB and DGSSA methods, when the number of iterations increases above a certain threshold value, the iteration procedure has a minor effect to the accuracy. The threshold value for DGSSA is 14, whereas for STMB it is 6.

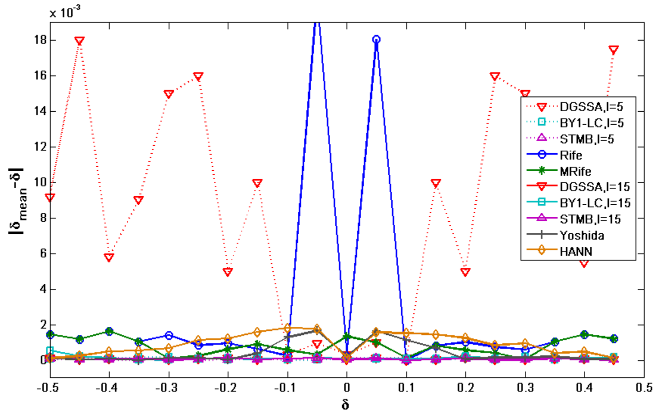

Fig. 5. The mean bias of frequency estimation as a function of δ change in the interval δ = [–0.5:0.05:0.45].

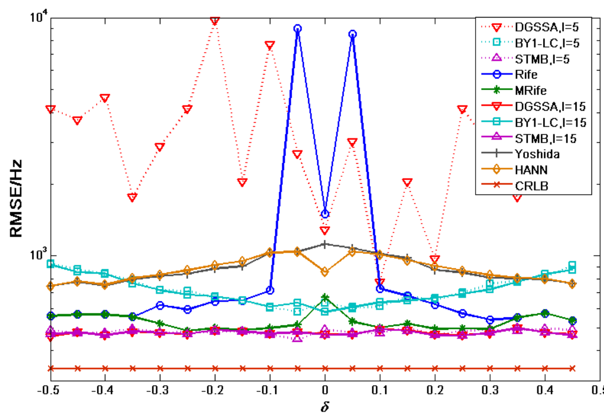

Fig. 6. The RMSE of frequency estimation as a function of δ change in the interval δ = [–0.5:0.05:0.45].

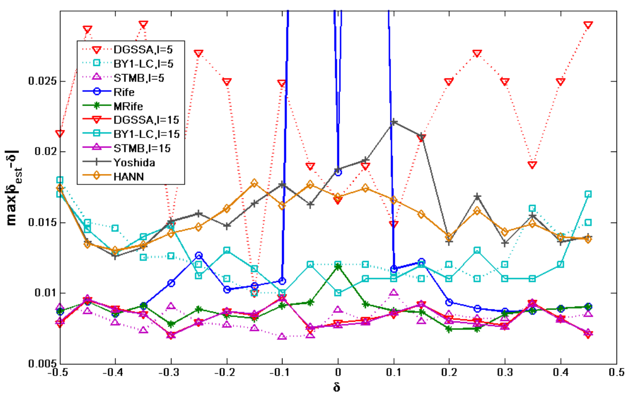

Fig. 7. The maximum modulus of the absolute error of δ estimation as a function of δ change in the interval δ = [–0.5:0.05:0.45].

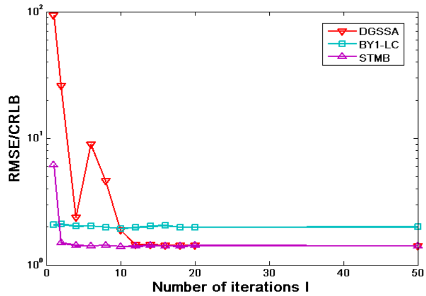

Fig. 8. The convergence with different numbers of iterations.

4.2. Signal to noise ratio analysis

To evaluate the immunity to noise of the proposed algorithm, signals containing noise with a random uniformly distributed phase from 0 to 2π are generated. *SNR* varies from 0 dB to 40 dB with the step of 4 dB. Fig. 9a and 9b compare the bias error and RMSE values which describe the errors on $\hat{\delta}$ of the proposed and other six methods for different *SNR* values.

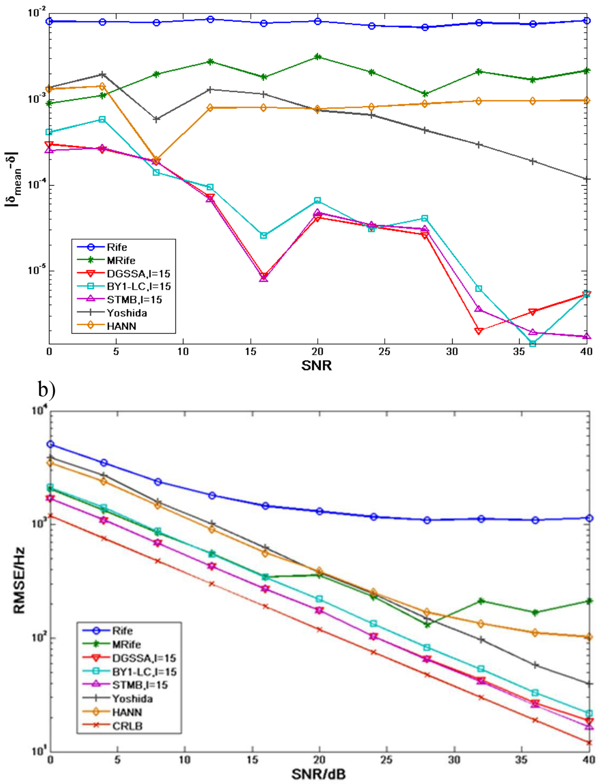

Fig. 9. Comparison of the bias error and the standard deviation of frequency estimation with observed samples (J = 43, δ = 0.008) vs. *SNR* with 1000 simulations, N = 1024, f_s = 100 MHz. a) the bias error as a function of *SNR*; b) the standard deviation of frequency estimation as a function of *SNR*.

In this figure, the parameters J and δ are fixed to specific values, which are $J = 43$, $\delta = 0.008$. For each value of *SNR*, 1000 runs with $f_s = 100$ MS/s, $N = 1024$, and 15 iterations are analyzed.

As expected, with increasing the noise level, performance of considered methods deteriorates. It is seen from Fig. 9 that, except the Yoshida method, for other non-iteration DFT-based methods the RMSE values of the estimation errors go away from the CRLB when *SNR* increases. That is because the spectral leakage dominates over the noise level. Fig. 9 shows that the least biased estimators are the proposed DGSSA and STMB with 15 iterations (This is the general truth for any *SNR*.). By using DGSSA and STMB, we can observe that the RMSE of frequency estimates decreases linearly as *SNR* increases, with almost the same slope of CRLB. As can be observed in this figure, the mean values of RMSE for DGSSA (I = 15) and STMB (I = 15) are roughly equal to 1.4 times of CRLB. However, the RMSE for BY1-LC (I = 15) is 1.8 times of CRLB.

By using DGSSA, not only the frequency but also the other three parameters (amplitude, phase and dc component) of a single-tone sine wave can be estimated accurately. To prove it, these three parameters in this simulation are fixed to specific values, which are $A_v = 5$, $\varphi = \pi/3$ and $C = 0$. All other parameters are set as the same as in Fig. 9. Fig. 10 presents the absolute error and RMSE of these three parameters based on the proposed estimator. It can be seen that the RMSE values of these three parameters have a similar slope of frequency estimation.

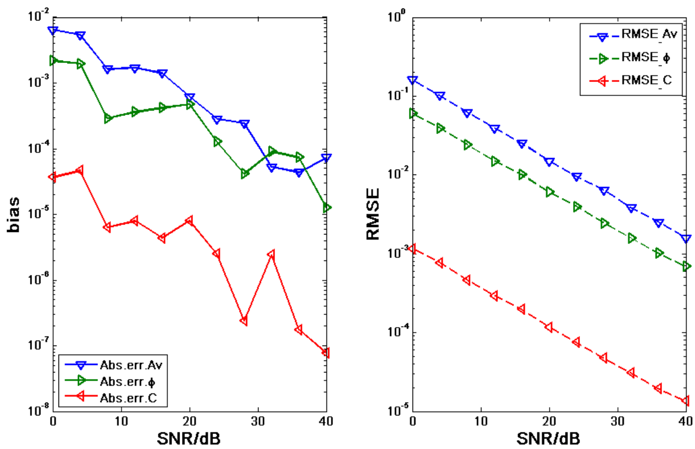

Fig. 10. The estimation performance of three parameters with DGSSA vs. *SNR*.

4.3. Sample number analysis

The sinusoidal signals considered in the following analysis are affected by the number of samples N. For a small N, the systematic errors due to a lower frequency resolution become smaller than the errors due to noise, and the accuracy of the proposed frequency estimator is shown in Fig. 11. The parameters are set as follows: $f_s = 100$M S/s, $f_c = 4.2$ MHz, $N_1 = 32$, $N_2 = 64$, $N_3 = 128$, $N_4 = 256$, $N_5 = 512$, $N_6 = 1024$, $N_7 = 2048$ and $SNR = 40$ dB. For each N, 1000 runs are done. All other parameters are set as in Fig. 9.

Figure 11 shows the absolute errors and RMSE values of estimated frequency obtained by different methods as functions of numbers of samples N. It can be observed that the RMSE values of estimators decrease as N increases. It can be seen that the best estimates are in all cases obtained by using iterative DFT-based algorithms. Because of a low frequency resolution, the accuracy of estimators for non-iterative DFT-based methods is deteriorated as N decreases. For any considered value of N, DGSSA and STMB can give more accurate results. When $N =$

16, that is $J = 0$, $\delta = 0.672$, the RMSE of DGSSA (I = 15) is 2.8 times of CRLB. However, when N is 32 ($J = 1$, $\delta = 0.344$), the RMSE of DGSSA (I = 15) is about 1.4 times more than CRLB with $SNR = 40$ dB. When N is 2048 ($J = 86$, $\delta = 0.016$), the RMSE of DGSSA (I = 15) is about 1.47 times more than CRLB. It can be concluded that the tendency of RMSE of DGSSA is consistent with CRLB when N is larger than 16. Furthermore, it keeps a relatively constant distance from CRLB. In addition, because of integer period truncation in windowed interpolation, the FFT algorithms, Yoshida IpDFT, and IpDFT with HANNING window algorithms are not suited for frequency estimation of partially periodical samples. As shown in Fig. 11, for $N = 16$（$J = 0, \delta = 0.672$）the estimated frequency cannot be realized by the IpDFT with Hanning window and Yoshida algorithms. The results presented in Fig. 11 show that the proposed method can work with a very small number of signal cycles, in contrary to some other competitors.

Figure 12 shows how the computational requirements of the proposed algorithm depend on the number of samples N of the processed signals.

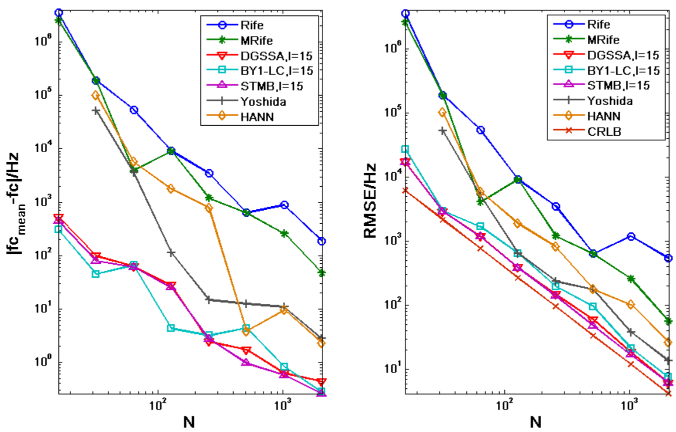

Fig. 11. The performance of DGSSA with different numbers of samples (SNR = 40dB).

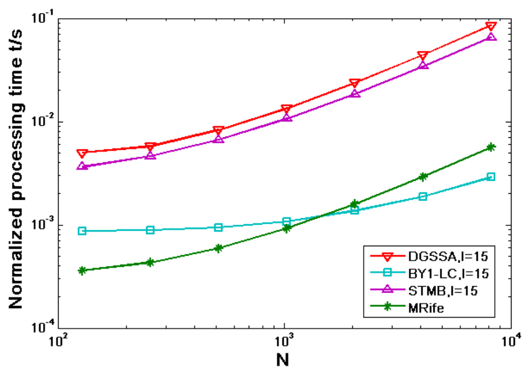

Fig. 12. The normalized processing time versus the number of samples.

It can be concluded that increasing the number of samples N in the BY1-LC method does not need more computation time. BY1-LC may be less complex than STMB because it only needs to compute the correction for three DFT bins in each iteration step. In addition, the STMB algorithm and the DGSSA algorithm have the same change trend as N is increasing. However, with a larger number of *N*, the matrix decomposition of three-parameter fitting needs more processing time in DGSSA.

5. Conclusion

In this article, we have reviewed estimation of the frequency of a single-tone sine under the condition of noise. The robustness, accuracy, convergence, noise immunity and computation complexity of the proposed estimator are compared with many methods by many MATLAB simulations. The remarkable feature of the proposed DGSSA method is obtained by the golden section searching algorithm using three DFT spectral samples. By increasing the iteration time, better results are obtained at the cost of a higher computational complexity in the proposed method. The RMSE of MRife and BY1-LC is larger than that of the STMB with the same number of iterations. As can be observed from simulations, the mean value of RMSE for DGSSA (I = 15) is roughly equal to 1.4 times of CRLB with *SNR* within the range of 0−40dB. However, compared with the STMB method, longer computation of DGSSA is required; however, the other three parameters of sine wave (amplitude, phase, and dc component) can also be evaluated accurately at the same time. So, the DGSSA algorithm may be a very good choice for a number of practical applications.

Acknowledgments

This work was financially supported by National Natural Science Foundation of China (No. 51275492), the International Science & Technology Cooperation Project of the Ministry of Science and Technology, People's Republic of China (No. 2010DFB10480).

References

[1] Borkowski, J. Kania, D., Mroczka, J. (2014). Interpolated-DFT-Based Fast and Accurate Frequency Estimation for the Control of Power. *IEEE Transactions on industrial Electronics*, 61(12), 7026–7034.

[2] Pantazis, D.Y., Rosec,O., Stylianou, Y. (2010). Iterative Estimation of Sinusoidal Signal Parameters. *IEEE Signal Processing Letters*, 17(5), 461–464.

[3] Robbins, PA. (1984). The ventilatory response of the human respiratory system to sine waves of alveolar carbon dioxide and hypoxia. *The Journal of Physiology*, 350, 461–474.

[4] Vanlanduit, R., Vanherzeele, J., Guillaume, P., Cauberghe, B., Verboven, P. (2004). Fourier fringe processing by use of an interpolated Fourier-transform technique. *Appl. Optics*., 43, 5206–5213.

[5] Candan, C. (2011). A Method For Fine Resolution Frequency Estimation From Three DFT Samples. *IEEE Signal Processing Letters*, 18(6), 351–354.

[6] Liao, J., Lo, S. (2014). Analytical solutions for frequency estimators by interpolation of DFT coefficients. *Signal Processing*, 100, 93–100.

[7] Aboutanios E., Ye, S. (2014), Efficient Iterative Estimation of the Parameters of a Damped Complex Exponential in Noise. *IEEE Signal Processing Letters*, 21(8), 975–979.

[8] Zieliński, T.P., Duda, K. (2011). Frequency and damping estimation method – an overview. *Metrol. Meas. Syst.*, 18(4), 505–528.

[9] Duda, K., Zieliński, T.P., Magalas, L.B., Majewski, M. (2011). DFT-based Estimation of Damped Oscillation Parameters in Low-frequency Mechanical Spectroscopy. *IEEE Trans. Instrum. Meas.*, 60(11), 3608–3618.

[10] Yoshida, Y.I., Sugai, T., Tani, S., Motegi, M., Minamida, K., Hayakawa, H. (1981). Automation of internal friction measurement apparatus of inverted torsion pendulum type. *J. Phys. E. Sci. Instrum*., 14, 1201–1206.

[11] Rife, D.C., Vincent, G.A. (1970). Use of the discrete Fourier transform in the measurement of frequencies and levels of tones. *Bell Syst. Tech. J.*, 49(2), 197–228.

[12] Zhenmiao, D., Yu, L. (2007). The Starting Point Problem of Sinusoid Frequency Estimation Based on Newton's Method. *Acta Electronica Sinica*, 35(1), 104–107.

[13] Xudong, W., Yu, L., Zhenmiao, D. (2008). Modified Rife algorithm for frequency estimation of sinusoid and implementation in FPGA. *Systems Engineering and Electronics*, 30(4), 621–624.

[14] Duda, K., Zieliński, T.P. (2013). Efficacy of the Frequency and Damping Estimation of a Real-Value Sinusoid Part 44 in a series of tutorials on instrumentation and measurement. *IEEE Instrumentation & Measurement Magazine*,16(2), 48–58.

[15] Steiglitz K., McBride, L.E. (1965). A technique for identification of linear systems. *IEEE Trans. Automatic Control*, (10), 461–464.

[16] Wu, R.C., Chiang, C.T. (2010). Analysis of the Exponential Signal by the Interpolated DFT Algorithm. *IEEE Trans. Instrum. Meas.*, 59(12), 3306–3317.

[17] *IEEE Standard for terminology and test methods for analog-to-digital converters*. (2000). IEEE Std. 1241.

[18] Bilau, T.Z., Megyeri, T., Sarhegyi, A., Markus, J., Kollar, I. (2004). Four-parameter fitting of sine wave testing result: iteration and convergence. *Computer Standards & Interfaces*, 26, 51–56.

[19] Andersson, T., Handel, P. (2006). IEEE Standard 1057, Cramer-Rao Bound and the Parsimony Principle. Instrumentation and Measurement. *IEEE Transactions On*, 55(1), 44–53.

[20] *IEEE Standard for Digitizing Waveform Recorders*. (2008). IEEE Std. 1057–2007.

[21] da Silva, M.F., Cruz Serra, A. (2003). New methods to improve convergence of sine fitting algorithms. *Computer Standards & Interfaces*, 25, 23–31.

[22] Bilau, T.Z., Megyeri, T., Sárhegyi, A. (2002). Four parameter fitting of sine wave testing results: iteration and convergence. *4th International Conference on Advanced A/D and D/A Conversion Techniques and their Applications, and 7th European Workshop on ADC Modelling and Testing*, Prague, Czech Republic, 1–5.

[23] Wilde, D.J., Beightler, C.S. (1967). *Foundations of optimization. Englewood Cliffs*. NJ: Prentice-Hall Inc.

[24] Wen-Chen, Y., Lun, Z., Qian, R., Meng, Z. (2013). Multi-objective Optimization for Traffic Signals with Golden Ratio Based Genetic Algorithm. *Journal of Transportation Systems Engineering and Information Technology*, 13(5), 48–55.

[25] Zhang, L., Zhang, M., Yang, W., Dong, D. (2015). Golden Ratio Genetic Algorithm Based Approach for Modelling and Analysis of the Capacity Expansion of Urban Road Traffic Network. *Computational Intelligence and Neuroscience*, 1–9.